Proceedings of DETC'00:
26th Biennial Mechanisms and Robotics Conference
Sept. 10-13, 2000, Baltimore, Maryland

DETC2000/MECH-14157

DESIGN AND CONTROL OF A SHAPE MEMORY ALLOY WIRE BUNDLE ACTUATOR

Michael J. Mosley[1] and Constantinos Mavroidis[2]
Robotics and Mechatronics Laboratory
Department of Mechanical and Aerospace Engineering
Rutgers University, The State University of New Jersey
98 Brett Road, Piscataway, NJ, 08854-8058
Tel: 732-445-0732, Fax: 732-445-3124
E-mail: mavro@jove.rutgers.edu

ABSTRACT

In this paper, the design and control of a novel shape memory alloy (SMA) actuator that possesses impressive payload lifting capabilities are presented. The actuator consists of 48 nickel-titanium SMA wires mechanically bundled in parallel forming one powerful artificial muscle. This new linear actuator can apply up to 100 lb_f (445 N), which is approximately 300 times its weight, over a maximum distance of 0.5 in. (1.27 cm). The actuator was tested in two different loading configurations – linear displacement and operation of a revolute joint. A PID based controller with the addition of an input shaping function was developed for each loading configuration with excellent results, maintaining steady state error within ± 0.004 in. (0.1 mm) for linear motion and ± 1° for revolute joint rotation. This powerful, compact, and lightweight actuator shows promise for use in space, medical, and other macro-robotic applications.

1 INTRODUCTION

The goal behind the research discussed in this paper is to develop a new generation of large-scale robotic systems that are much lighter, and more compact than existing systems, but still retain the strength to perform the assigned task. Advances in material technology have introduced lightweight substances, making it possible to build structurally strong actuation mechanisms that are compact and weigh very little. However, conventional actuators, such as electric motors and hydraulic and pneumatic cylinders, prevent large reductions in the overall weight and complexity of robots. Examples of two industries that would benefit from a new type of actuator are space exploration and prosthetics.

In this work, the key methodology employed to drastically reduce the weight and complexity of robotic systems is the use of Flexinol™ nickel-titanium (Ni-Ti) shape memory alloy (SMA) wires as actuators of the robot joints. Flexinol™ wires, made by Dynalloy, Inc., have the property of shortening up to 8% of their length when heated and thus are able to apply forces. This phenomenon, called the shape memory effect (SME), occurs when the material is heated above a certain transition temperature changing its phase from martensite to austenite. Heating, and thus contraction, of a Flexinol™ actuator is easily accomplished by applying a voltage drop across the wire causing current to flow through the material, resulting in joule heating. Ease of actuation is not the only advantage of Ni-Ti SMA actuators. When compared to other actuators, they possess the highest power to weight ratio for those weighing less than 1 lb. (0.45 kg) [1]. Other advantages are their incredibly small volume and low cost.

Since 1983, Ni-Ti SMA actuators, have been used in micro-robotics [2]. It was discovered that the motion of actuators fabricated from this material could be controlled and that their small size and displacement was ideal for micro-

[1] Graduate Student
[2] Assistant Professor, ASME Member, Corresponding Author

robots (i.e. robots on a millimeter scale). In this context, Ni-Ti SMA has been used in many different robotic systems as micro-actuators [3-7]. A detailed review of the literature on SMA actuators can be found in [8]. Although there has been significant research into using Ni-Ti SMA actuators in small robotic systems, their use in larger robotic systems has been very limited. The primary reasons are the small linear displacement capability and absolute forces obtained from one wire.

This paper presents the design and control of a new and powerful Ni-Ti SMA based actuator that can apply very large forces and thus can be used to operate the joints of macro-robotic mechanisms. Large forces are achieved by "bundling" a set of Ni-Ti wires, thus increasing the power of the actuator. A SMA Bundle consisting of 48 Flexinol™ wires was constructed and actuated by a computer-controlled electrical circuit. This actuator was designed to apply up to 100 lbs. (445 N), approximately 300 times its weight, over a maximum distance of 0.5 in. (1.27 cm). As far as the authors are aware, this is the first SMA wire bundle actuator with such force capabilities. In order to determine the performance characteristics of the SMA Bundle, an instrumented test rig was designed and constructed. This setup was equipped with a load cell, linear displacement sensor, current and voltage sensors, and a thermocouple central to the bundle. Open and closed loop experiments were conducted on the SMA Bundle with two different loading configurations – linear displacement and operation of a revolute joint. A PID based controller with the addition of an input shaping function was developed for each loading configuration with excellent results, maintaining steady state error within ± 0.004 in. (0.1 mm) for linear motion and ± 1° for revolute joint rotation. Here, the SMA bundle design and results of closed loop control experiments are discussed. Results of the open loop experiments are described in [9].

2 DESIGN CONSIDERATIONS

In order to augment the force capabilities of SMA wire actuators, the overall cross-sectional area of the SMA material normal to the direction of actuation must be increased. This can be achieved in two different ways – using thicker wires or connecting many wires mechanically in parallel. Although both of these methods achieve the goal of a more powerful actuator, there are other consequences that must be considered. Actuator bandwidth and power supply requirements are dramatically altered by changes in cross-sectional area and these effects must be taken into account.

One of the parameters that greatly affects the bandwidth of a Flexinol™ wire actuator is the diameter. The physical reason behind this behavior is the change in surface to volume ratio and thus the change in the heat transfer characteristics of the setup – the larger the surface to volume ratio, the greater the heat transfer, and the larger the bandwidth. So, in order to improve the force capabilities of a SMA actuator while not sacrificing bandwidth, it is more beneficial to use many thin wires connected mechanically in parallel rather than a single thick wire. Not only must thin wires be used, but they also must remain separated so that the cooling medium, in this case air, can flow freely around all surfaces. One can think of this situation as analogous to the cooling tubes in a condenser where a large number of tubes are used to increase the heat transfer surface area. On the other hand, if many small wires were gathered together like the fibers in a rope, the advantages of the increased surface area would not be realized.

Initially, one may think that the best circuit design for the bundle itself is a parallel arrangement of the wires similar to how they are mechanically arranged. Although this is the simplest arrangement, it results in impractical power supply requirements due to the low resistance. As an example, the effective resistance of a bundle consisting of 50, 12 in. (30.5 cm) long, 0.006 in. (150μm) diameter wires all in parallel would be 0.305Ω. Given a required actuation current of 0.4 amps through each wire (20 amps for the whole bundle), the resulting voltage drop across the bundle is 6.1 V. (The required actuation current for each wire, 0.4 amps in the case of a 0.006 in. Flexinol™ wire, is the current needed to cause complete contraction in one second when surrounded by room temperature air.)

This combination of low voltage and very high amperage can be avoided by creating a circuit where the wires are arranged electrically in a combination of series and parallel paths while remaining mechanically connected in parallel. For a combination of wires in series and parallel:

$$V_B = I_{SMA} \bullet \frac{N}{P} \bullet L \bullet \overline{R} \quad \text{and} \quad I_B = P \bullet I_{SMA} \quad (1)$$

where V_B and I_B are the voltage drop across and current through the bundle, I_{SMA} is the single wire actuation current, N is the number of wires in the bundle, P is the number of parallel paths, L is the bundle length, and $\overline{R}$ is the single wire linear resistance. Note that the ratio N/P must be equal to an integer if identical paths are constructed. For the case where there are 48, 0.006 in. (150μm) wires, Figure 1 shows a plot of current and voltage requirements in order to achieve actuation current (0.4 amps) in each wire for different numbers of parallel paths.

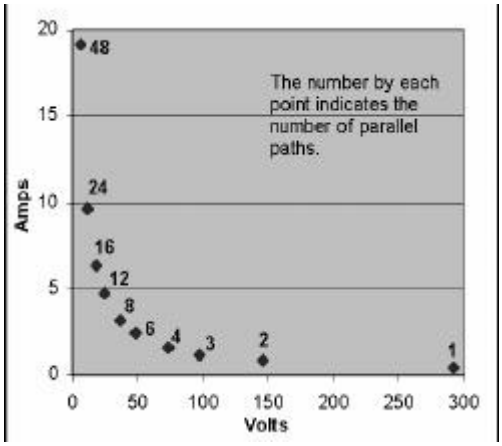

Figure 1: SMA Bundle Current vs Voltage

In 1984, a SMA servo-actuator was designed using four SMA elements mechanically connected in parallel and electrically connected in series [10]. The benefits of a lower current requirement, higher voltage requirement, and improved heat transfer over a single thicker wire were realized. However,

if a large number of SMA elements, say 48, are connected completely in series (one parallel path), the required voltage for actuation becomes very large (see Figure 1). Using different numbers of parallel paths allows the bundle to be tailored to different applications where there may be current or voltage restrictions.

Considering the above discussion, SMA Bundle design has four key parameters that determine the load capability, displacement capability, and current/voltage requirements. These parameters are diameter of the wire, the number of wires, the length of the bundle, and the number of parallel current paths.

3 SMA BUNDLE EXPERIMENTAL SET-UP

The goal in this work was established to design an actuator that can apply a maximum of 100 lb_f (445 N) over a distance of approximately 0.5 in. (1.27 cm). A SMA Bundle actuator with these capabilities will be able to power a revolute joint moving a lever arm that can lift and rotate approximately 5 pounds of weight (2.3 kg) at the end of the arm through an angle of 90º. Demonstrating such payload and angular displacement capability from an SMA actuator will show that such actuators can be used effectively in macro-robotic applications.

Given that Flexinol™ wires can contract 5 to 8% of their original dimension, a bundle length of 12 in. (30.5 cm) was chosen to meet the displacement criterion. Simple experiments were conducted to determine the weight lifting capability of different diameter Flexinol™ wires. It was found that a single 0.006 in. (150μm) wire could lift over 2 lb. (0.9 kg) and possessed a sufficiently rapid cycling time for application in a prototype bundle. Considering that one wire can lift over 2 lb., in theory, fifty 0.006 in. wires connected mechanically in parallel could lift at least 100 lb. In the end, 48 wires were used due to the symmetry of arrangement into a cylindrical bundle.

A SMA Bundle was constructed consisting of 48, 12 in. (30.5 cm) long, 0.006 in. (150 μm) diameter wires (N=48, L=12 in). The 48 wires were connected mechanically in parallel between two 0.25 in. (0.635 cm) thick, 1.5 in. (3.81 cm) diameter virgin Teflon end plates. Teflon was selected due to its high dielectric strength, temperature resistance, and good mechanical stability. Since all wires were not at the same voltage (series/parallel arrangement), it was necessary to keep each one electrically isolated from the others at the bundle end plates. Each wire passed through the end plate and was terminated with a 1/32 in. (0.079 cm) copper crimp, providing an excellent mechanical and electrical connection (see Figure 2). The copper crimps fit tightly into 48 sockets machined into each end plate.

In order to determine the performance characteristics of the SMA Bundle, an experimental setup was designed and constructed (see Figure 3). The experimental setup consisted of 4 main parts: a) the test rig composed of the frame, the SMA Bundle, the load, and various electrical power connections, b) the power supply, c) the control and instrumentation unit, and a PC. The test rig frame provides a hanging point for the upper end of the SMA Bundle. The lower/free end of the vertically oriented bundle is connected to the load. In the linear loading configuration, a variable weight and/or springs can act as the SMA Bundle load.

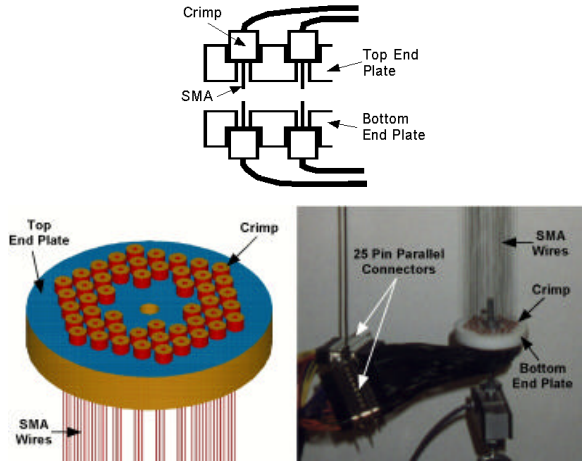

Figure 2: Crimping Schematic and Bundle Assembly

In order to vary the number of parallel electrical paths through the SMA Bundle, a "patch terminal" system was setup. The Patch Terminals consist of four 48-pin cannon plugs. A set of short patch wires was used to create the desired current path through the bundle. For all of the experiments conducted in this research, the patch terminals were wired for 8 parallel paths with 6 wires in series for each parallel path. As shown in Figure 2, this results in a theoretical actuation voltage of 36.6 volts and a current of 3.2 amps for complete contraction of the bundle in one second.

The Power Supply for bundle actuation was a Tellabs 48 V (nominal), 10 amp DC power source The raw voltage from the power supply was controlled using a custom designed operational amplifier circuit. The custom circuitry was based around a Burr Brown OPA 512 Power Operational Amplifier. The gain of the amplifier was set to 10 so that a 0 to 5 V input signal resulted in 0 to 50 V applied to the SMA Bundle. A 350 MHz Dell PC was used for data acquisition and closed loop control running our Windows NT based real time control software named WinReC v.1.

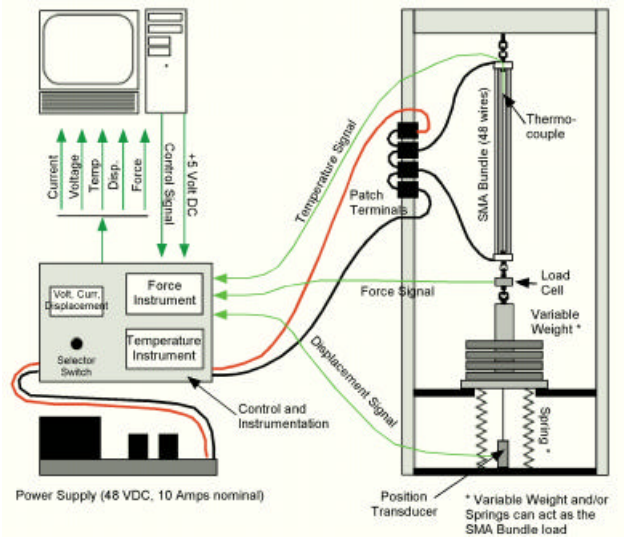

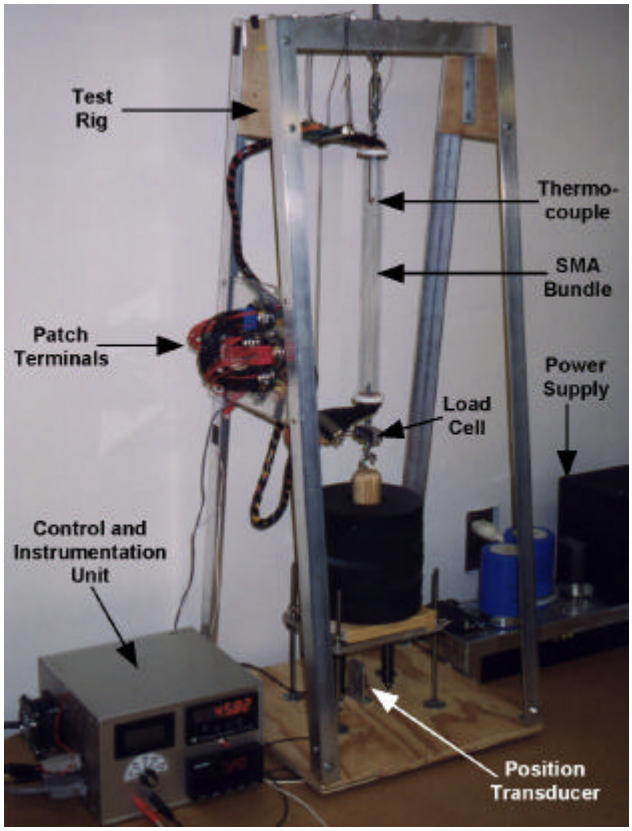

Figure 3: SMA Bundle Experimental Setup

Since the majority of robotic systems consist of links that rotate about revolute joints, it was also desired to test the performance of the SMA Bundle while actuating a revolute joint. A schematic of this mechanism is illustrated in Figure 4.

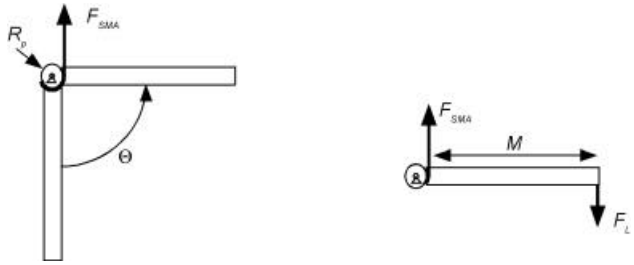

Figure 4: Cable and Pulley Mechanism

The SMA actuator pulls on a small, flexible cable that wraps around and fastens to a pulley fixed to the moving link. For a constant load, the relationship between the required pulley radius, R_p, the maximum SMA deflection, Δ_{SMA}, and the desired angular deflection of the moving link, Θ, is:

$$R_p = \frac{D_{SMA}}{Q} \tag{2}$$

Clearly from this relationship, for large angular deflections, R_p must typically be small compared to the length of the moving link, M. Considering a static problem, the resulting ratio of required actuation force, F_{SMA}, to the load, F_L is:

$$\frac{F_{SMA}}{F_L} = \frac{QM}{D_{SMA}} \tag{3}$$

The next step was to design a modification to the existing experimental setup allowing the incorporation of a cable and pulley SMA actuated revolute joint. The goal was established to lift and rotate approximately 5 pounds of weight (2.3 kg) through an angle of 90º. Based on the results of the open loop experiments in the linear configuration, the maximum contraction, Δ_{SMA}, was assumed to be 0.4 in. (1 cm). A conservative estimate of 80 lb_f (356 N) was made for the maximum bundle force, F_{SMA}. Using Equation 2 and 3, the pulley radius, R_p, was found to be equal to 0.225in (0.648cm) and corresponding lever arm, M equal to 4.07in (103cm).

Upon achieving the appropriate parameter values, the revolute mechanism shown in Figure 5 was designed and assembled. The revolute joint is composed of a steel axle supported at each end by a radial ball bearing mounted in square aluminum bar stock. The bars fasten to the vertical steel posts that originally guided the linear load when in the linear loading configuration. The lever arm is fastened to the axle and provides a threaded connection to attach different sized loads. A 0.25 in. (0.635 cm) radius power pulley was fastened to the axle. The SMA Bundle was attached to the power pulley using a special grade anti-stretch cable at a point that allowed at least 90° rotation. The 0º position of the joint is defined by the arm pointing straight down.

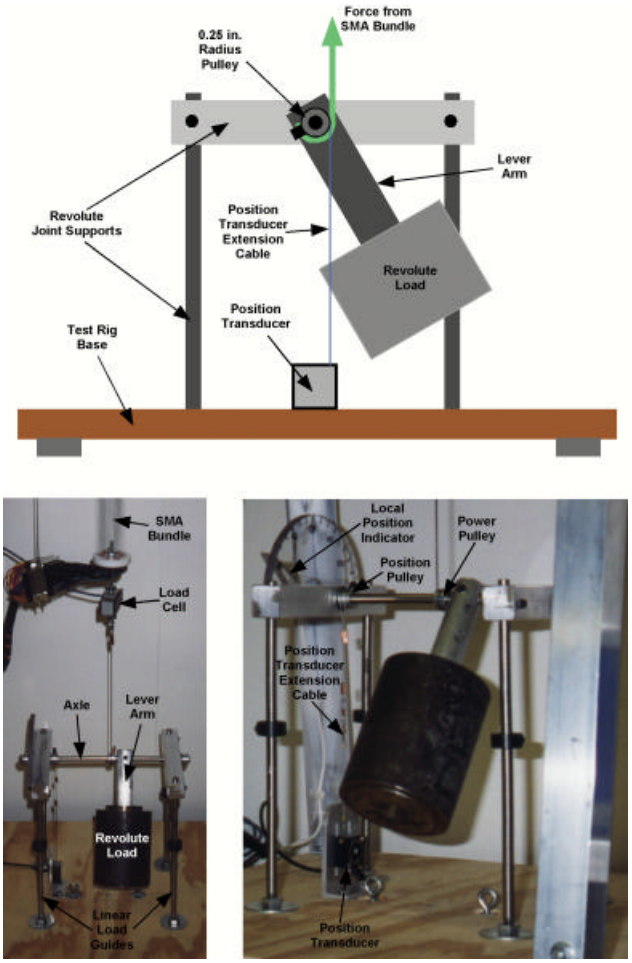

Figure 5: SMA Bundle Actuated Revolute Joint

4 CLOSED LOOP CONTROL

4.1 Linear Loading Configuration

Initially, a classical PID controller was developed to guide the SMA Bundle as it lifted a weight. The following control law was used:

$$V_{CC} = K_P e(t) - K_D \frac{dx(t)}{dt} + K_I \int_0^t e(t)dt \qquad (4)$$
$$if \;\; V_{CC} > 50 \;\; then \;\; V_{CC} = 50$$
$$if \;\; V_{CC} < 0 \;\; then \;\; V_{CC} = 0$$

where: V_{CC} is the calculated control voltage, K_P, K_D, and K_I are the proportional, differential, and integral gains, $e(t)$ is equal to $x_d(t)$-$x(t)$ where $x_d(t)$ is the desired position, and $x(t)$ is the actual position. The conditional statement for $V_{cc}>50$ defines the saturation of the power supply.

Using a trial and error procedure the controller gains were selected at K_P = 110, K_I = 75, and K_D =10. For these gains, a set of step input responses, are shown in Figure 6. For this set of gains, the controller did not saturate, and thus the control voltage was a smooth function of time. Since there was no sharp change in control voltage, the rate of SMA Bundle contraction changed smoothly and harmonic vibration was not initiated. For the typical response, the maximum steady state error was approximately ± 0.01 in. (± 0.254 mm). It is of particular concern that the SMA Bundle controller be very accurate since inaccuracies in the linear configuration are amplified in the revolute joint configuration by a ratio of the link length, M, to the pulley radius R_P. This ratio is approximately 16 to 1 for the revolute loading mechanism constructed in this research.

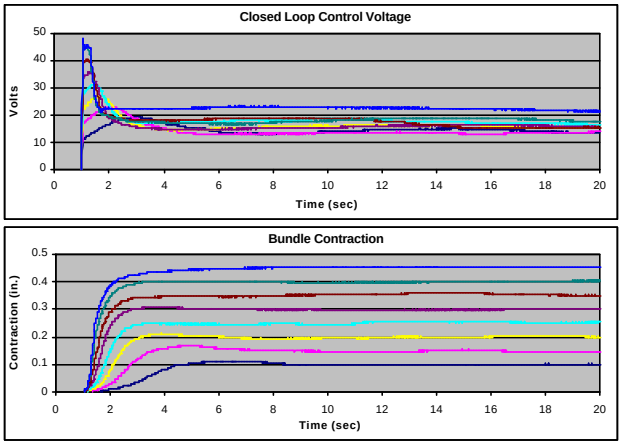

Figure 6: Classical PID Control of the SMA Bundle

The responses shown in Figure 6 were recorded in ideal environmental conditions with minimal disturbances. In a practical situation, changes in the temperature and velocity of the medium surrounding the bundle would result in thermal disturbances. Figure 7 displays the controller's ability to reject thermal disturbances created by rapidly waving a stiff piece of cardboard near the bundle for approximately ½second. The initiation of each disturbance is marked on the plot with arrows. Note the large position excursion that occurs due to the small, short duration disturbance and that the controller takes over two seconds to correct the error. Mechanical disturbance tests were also run showing the poor performance of this controller in rejecting mechanical disturbances.

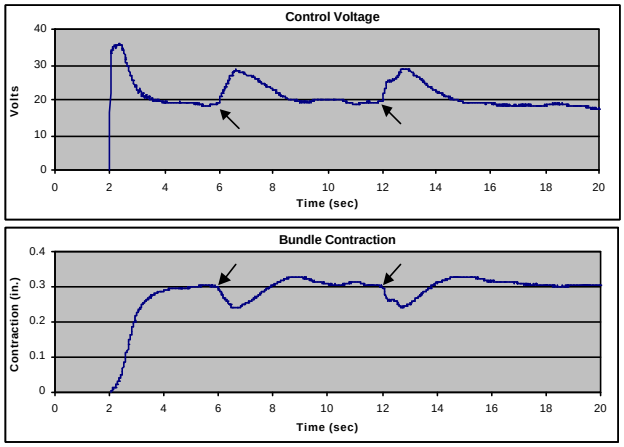

Figure 7: Thermal Disturbance Rejection Tests

Although the controller presented above produced a smooth response to step inputs, it is clearly not suitable for high accuracy, rapid tasks in a disturbance filled environment. The controller gains need to be set higher for faster responses and better disturbance rejection. However, higher gains tend to saturate the controller during initial response to a step input and initiate harmonic vibration when the control voltage rapidly drops from saturation.

In order to eliminate the performance problems when higher gain controllers are used, the output of the standard PID controller was shaped using an exponential function. The goal was to smooth the voltage transition when exiting or approaching the saturation limit. The exponential shaping function was used to: 1) define the saturation limit when V_{CC} was large and 2) approximate V_{CC} when in the range of typical voltages needed to hold a certain position. The net effect was to reduce the gains for large V_{CC} and return the gains to near their original value when holding a certain position. The PID control law combined with this "exponential saturation" function is the following:

$$V_{CC} = K_P e(t) - K_D \frac{dx(t)}{dt} + K_I \int_0^t e(t)dt$$
$$V_{CM} = V_S(1 - e^{-aV_{CC}}) \qquad (5)$$
$$if \; V_{CM} < 0, \quad V_{CM} = 0$$

where V_{CM} is the modified control voltage, V_S is the desired saturation voltage, and a is a factor that determines the shape of the "exponential saturation" curve. Larger values of a make the curve steeper for low values of V_{CC}. An example of "shaping the control input" with this method is shown in Figure 8. For the typical range of voltages needed to hold a certain position (10 to 20 volts) the "exponential saturation" curve approximates the calculated control voltage. As the calculated control voltage gets higher, the "exponential saturation" curve approaches the desired saturation limit.

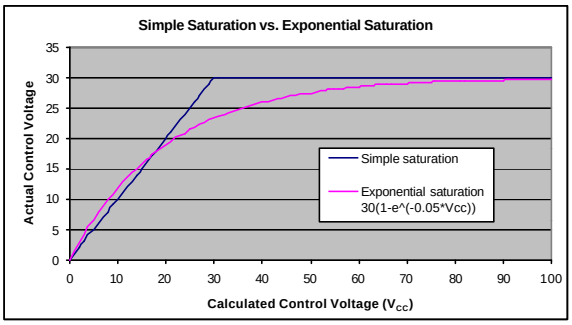

Figure 8: Comparison of Control Inputs

When "exponential saturation" was applied to the PID controller, high gains could be set without generating large vibrations. Figure 9 shows the system responses to a set of step inputs where the controller in Equation 5 is defined by: K_P = 1500, K_I = 1000, K_D = 50, V_S = 30, and a = 0.05.

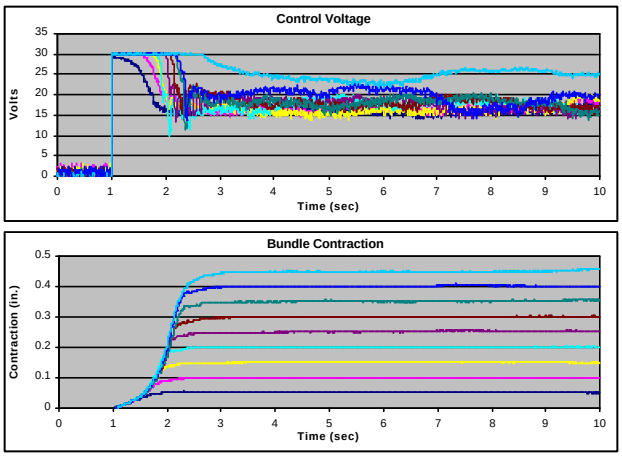

Figure 9: Modified PID Control of the SMA Bundle

With higher gains, disturbance rejection was greatly improved. Figure 10 shows the controller rejecting four thermal disturbances of similar magnitude to the ones in Figure 7. The errors are about 1/3 the size of those in Figure 7 and are corrected in less than one second.

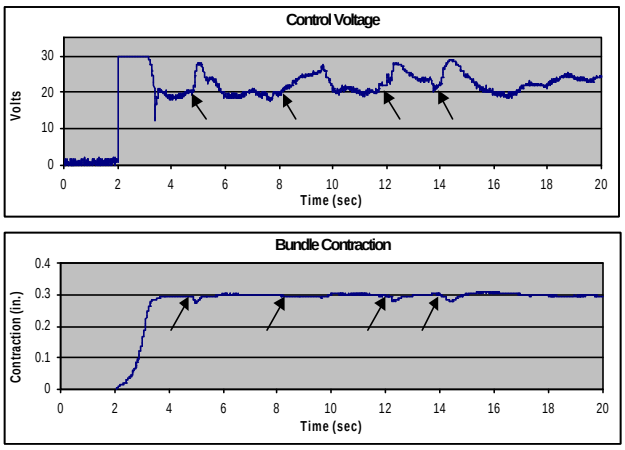

Figure 10: Thermal Disturbance Rejection Tests

4.2 Revolute Joint Loading Configuration

The experimental setup was shifted to the revolute joint loading configuration and closed loop control of joint position was examined. A controller was developed based on Equation 5. Due to the elasticity of the system and the low friction design, some form of damping in both ways of motion was needed to obtain an acceptable response in closed loop control. Since active damping in both motion directions would require a major revision of the existing experimental setup and addition of a second bundle, the option of passive damping by incorporating a mechanical dissipative device into the revolute joint was investigated first. A commercially available rotational damper was introduced in the experimental setup. A representative system response obtained is presented in Figure 11 where the controller was defined by the following: K_P = 20, K_I = 8, and K_D = 6, V_S = 35, and a = 0.05. The controller was able to reach and hold the desired position to within ±1° without oscillation. However, due to the added damping, the response was slow. The rise time of the system was limited by the force capability of the SMA Bundle. With gains large enough to give good disturbance rejection, the primary controller parameter that determined the bundle force during actuation was the exponential saturation voltage, V_S. Values of V_S greater than 35 volts resulted in too rapid heating and contraction of the SMA wires, causing rapid rotation of the joint and a correspondingly large counter torque applied by the damper. As a result, large bundle loads occurred. The bundle force plot in Figure 11 shows the large loads that occurred when V_S was set to 35 volts. Here, the force approached 75 lb. (334 N) whereas without damping, a maximum of only 32 lb. (142 N) was needed to lift and rotate the 2.2 lb. weight.

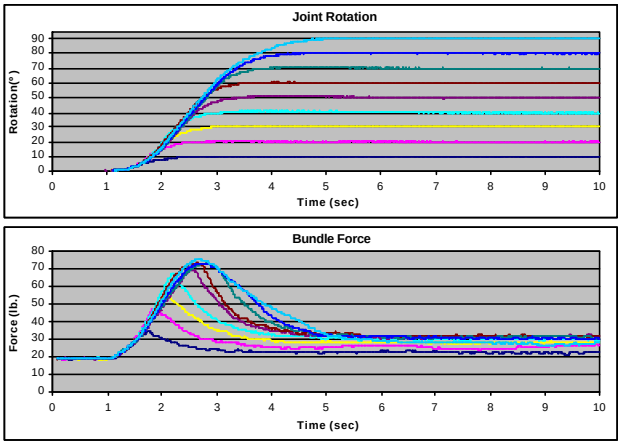

Figure 11: Modified PID Control of SMA Bundle Actuated Revolute Joint

As for the linear loading configuration, thermal and mechanical disturbance rejection tests were performed during closed loop control of the revolute joint. The combination of a high gain controller and a rotational damper resulted in excellent disturbance rejection. Figure 12 shows the system response to two thermal disturbances of similar magnitude and duration to those previously discussed (initiation marked by the arrows). The controller holds the error to within three degrees and is generally able to correct the error in under one second.

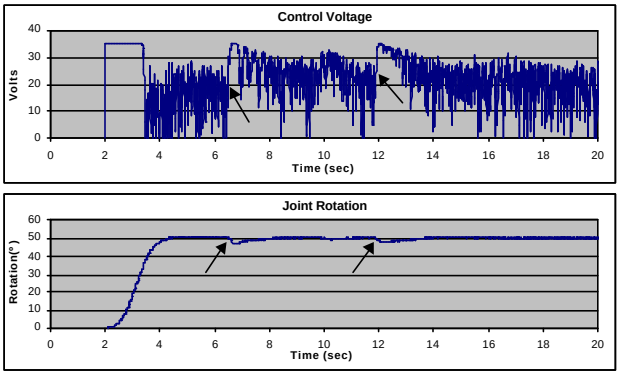

Figure 12: Thermal Disturbance Rejection Test

Figure13 illustrates the controller's ability to reject a mechanical disturbance. The disturbance was created by manually pressing on the lever arm of the revolute joint until the local force indication read approximately 50 lb. (222 N). The controller rejected the disturbance in the same way as for the linear loading configuration. As the additional force was applied, the error was limited to ±1°. Similar to mechanical disturbance rejection in the linear configuration, when the load was suddenly released and the elastic strain recovered, SMA Bundle extension was not controllable and occurred as a function of the restoration force and heat transfer.

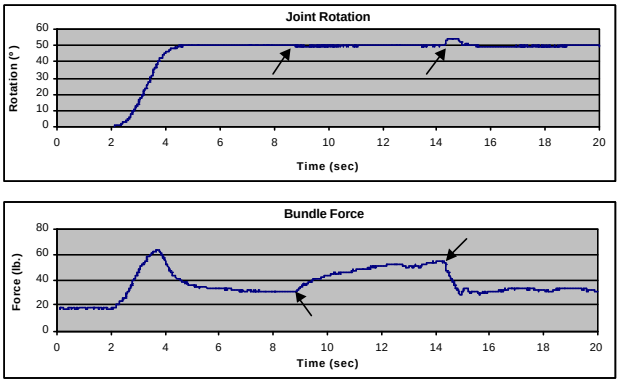

Figure 13: Mechanical Disturbance Rejection Test

5 CONCLUSIONS

The powerful, lightweight, and compact shape memory alloy wire bundle actuator designed, developed, tested, and controlled in this research provides a viable alternative to conventional actuators. It allows a method to drastically reduce the weight, complexity, and size of macro-robotic manipulators. As a linear actuator, the SMA Bundle was able to apply a maximum of $100lb_f$ (445 N) and contract up to 0.5 in. (1.27 cm). In the revolute joint configuration, the simple SMA Bundle actuated robotic system could lift and rotate up to 5 lb. of weight (2.3 kg) through 90° rotation. In both configurations, relatively simple PID based controllers with input shaping were able to hold a desired position with very good accuracy.

6 ACKNOWLEDGMENTS

The authors would like to thank the following organizations for their financial support for this project: Johnson and Johnson, Center for Computer Aids for Industrial Productivity, New Jersey Space Grant Consortium, and an Excellence Fellowship to Michael Mosley by the Rutgers University Graduate School.

7 REFERENCES

[1] Hirose, S., Ikuta, K. and Umetani, Y., 1989, "Development of a Shape Memory Alloy Actuators. Performance Assessment and Introduction of a New Composing Approach," Adv. Rob., 3(1), pp. 3-16.

[2] Honma D., Miwa Y. and Iguchi, 1985, "Micro Robots and Micro Mechanisms Using Shape Memory Alloy to Robotic Actuators," *J. Rob. Syst*., 2(1), 3-25.

[3] Caldwell, D. G., and Taylor, P. M., 1988, "Artificial Muscles as Robotic Actuators," *IFAC Robot Control Conf. (Syroco 88), Karlsrue*, Germany, pp. 401-406.

[4] Fujita, H., 1989, "Studies of Micro Actuators in Japan," *IEEE International Conference on Robotic Automation*, Vol. 3, pp. 1559-1564.

[5] Honma, D., Miwa, Y., and Igushi, N., 1989, "Micro Robots and Micro Mechanisms Using Shape Memory Alloy," *Integrated Micro Motion Systems. Micro-machining, Control and Application*, Nissin, Aichi, Japan, The 3rd Toyota Conference.

[6] Kuribayashi, K., 1986, "A New Actuator of a Joint Mechanism Using TiNi Alloy Wire," *International J. of Robotics Research*, Vol. 4, No. 4, pp. 47-58.

[7] Kuribayashi, K., 1989, "Millimeter Size Joint Actuator Using Shape Memory Alloy", *Sensors and Actuators*, Vol. 20, No. 1, pp. 57-64.

[8] Mavroidis C., Pfeiffer C. and Mosley M., 1999, "Conventional Actuators, Shape Memory Alloys and Electrorheological Fluids", Invited Chapter in *Automation, Miniature Robotics and Sensors for Non-Destructive Testing and Evaluation*, Y. Bar-Cohen (Ed.) http://cronos.rutgers.edu/~mavro/papers/ ch5-1-dinos-actuators3.PDF .

[9] Mosley M. and Mavroidis C., 1999, "Experimental Non-Linear Dynamics of a Shape Memory Alloy Wire Bundle Actuator", *Proc. of the 1999 ASME IMECE, Dyn., Meas. and Control Division*, Nashville, TE, Nov., 1999, Paper No. DSC-12B-1.

[10] Hirose, S., Ikuta, K., and Sato, K., 1989, "Development of a Shape Memory Alloy Actuator. Improvement of the Output Performance by the Introduction of a σ-Mechanism", *Adv. Rob.*, 3(2), pp. 89-108.